The Analyst

Piezoelectric mechanical pump with nanoliter per minute pulse-free flow delivery for pressure pumping in micro-channels

Satyajit Kar, Scott McWhorter, Sean M. Ford and Steven A. Soper*

Department of Chemistry, Louisiana State University, Baton Rouge, LA 70803-1804, USA.
E-mail: steve.soper@chemgate.chem.lsu.edu

A novel computer-controlled mechanical syringe pump is described which uses a piezoelectric actuator and a pivoted lever for amplification of the linear displacement of the piezo-actuator to deliver solvents free from pump pulsations at volumetric flow rates approaching 1 nl min^{-1} even at high loading levels (high output pressures). The flow patterns can be programmed by controlling the voltage waveform to the piezo-actuator to produce a linear displacement of 72 μm. By using the pivoted lever, a ninefold amplification of the piezo-expansion was achieved producing a total linear displacement of 648 μm. When a gas-tight glass syringe of 1.0 mm diameter was interfaced to the piezo-pump, the total volume delivered in a single pump stroke was 511 nl. Whereas the pumping profile was governed by the expansion behavior of the piezoelectric actuator, the flow rate was also slightly affected by the loading pressure on the pump as well. The piezo-pump was found to deliver adequately a stable flow of solutions with loading pressures as high as 3.79 $\times$ 10^5 Pa (actual loading pressure at the piezo-actuator = 3.41 $\times$ 10^6 Pa). Monitoring the flow stability using fluorescence indicated that the volume flow was fairly noise free at pumping rates from 4 to 150 nl min^{-1}. Below a volume flow rate of 4 nl min^{-1}, the pump exhibited extensive noise characteristics due to the step resolution of the DAC driving the piezo-actuator. A diffuser–nozzle system was fabricated which allowed automatic refilling of the syringe pump and was micromachined into Plexiglas (PMMA) using X-ray lithography. The diffuser–nozzle system contained channels that were 50 μm in depth and tapered from 300 to 30 μm. The diffuser–nozzle system was interfaced to the syringe pump by connecting conventional capillary tubes to the PMMA-based diffuser–nozzle, the piezo-pump and the chemical analysis system.

Keywords: *Piezoelectric actuator; syringe micropump; diffuser/nozzle; micromachining*

There is currently a pressing need for mechanical pumping devices that can deliver small volumes of materials (liquids or gases) at controlled rates with volumetric delivery rates in the low to sub nl min^{-1} range. Not only is it necessary to possess the ability to pump at low volumetric flow rates, but also the pump should be able to operate effectively when the pressure drop is large. For example, in the biomedical area, small and compact pumps can be used for administering drugs for the treatment of such diseases as diabetes. In analytical chemistry, pumps which can deliver low volumetric flow rates can be used for micro-liquid chromatography[1] and micro-dialysis.[2]

Recently, several research groups have focused on the development of miniaturized chemical analysis systems that can perform several different analytical techniques, such as separation *via* electrophoresis or chromatography, sample preparation and, finally, sample detection.[3–18] These devices consist of a series of channels with dimensions in the range 20–40 μm lithographically fabricated in glass or plastic materials. While most of the micro-fluidics in these devices have been accomplished *via* electropumping produced by electroosmotic flows generated in these micro-devices when fabricated in glass substrates, mechanical pumps will need to be developed which can be used in devices where the magnitude of the electroosmotic flow is insufficient to allow facile pumping. For example, when predominantly organic run buffers are used in the micro-electrophoretic format, the magnitude of the electroosmotic flow may be insufficient to allow facile electropumping.[19] In addition, we have developed miniaturized chemical analysis systems in Plexiglas [PMMA, poly(methyl methacrylate)] using X-ray lithography and determined that the small electroosmotic flow generated in these devices will require an external pumping source in some cases to move fluids at reasonable linear velocities.[20]

Since these miniaturized chemical analysis systems possess ultra-small channels, micro-pumps must be developed which can deliver fluids at very low volumetric flow rates to obtain reasonable linear velocities. In Fig. 1 is shown the calculated volumetric flow rate *versus* linear velocity through circular tubes with various diameters (10, 20 and 50 μm id). As can be seen, to obtain a linear velocity of 0.01 cm s^{-1} in a 10 μm id channel, a volumetric flow rate of 450 pl min^{-1} is required.

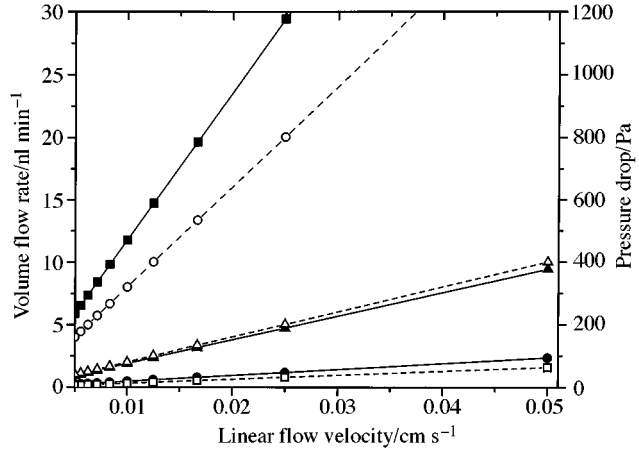

Fig. 1 Volume flow rate (solid lines, closed symbols) and pressure drop (dashed lines, open symbols) as a function of linear flow velocity. The volume flow rate and pressure drop were calculated assuming that pumping was occurring through a circular capillary tube of id 10 μm (circles), 20 μm (triangles) and 50 μm (squares) with a length of 10 cm. The solution viscosity was assumed to be 1 cP.

Another concern associated with pumping liquids through narrow bore channels is the pressure drop created by the small diameter and, as such, the micro-pump should be able to drive solutions adequately through these tubes when operated with high load pressures. In Fig. 1 is also shown the pressure drop across a micro-tube generated under different linear flow velocities. For example, a micro-tube possessing 10 μm id with a total length of only 5 cm and pumping water (viscosity = 1 cP) at a linear velocity of 0.01 cm s^{-1} results in a pressure drop of approximately 450 Pa. Therefore, one can see that micro-fluidic pumping in small id channels requires a mechanical pump that can operate reasonably well at high load pressures and also demonstrate stable flows at low volumetric rates.

Micro-mechanical pumps can also find applications in systems where it becomes necessary to transfer small volumes (picoliter to nanoliter) of material into micro-reactors for sample preparation utilized in miniaturized chemical analysis systems. An example is a genetic analysis system that we are currently constructing which involves the restriction digestion of DNA samples in an enzyme micro-reactor possessing a total volume of approximately 20–30 nl and transferring this minute sample to an electrophoresis separation channel for fractionation. Since the handling of nanoliter volumes of samples can be problematic, the enzyme reactor is incorporated on-line with the electrophoresis separation device. Prior to separation, intact DNA molecules are subjected to enzyme catalyzed fragmentation. Based on our experience, the residence time of the DNA sample in the micro-reactor required to achieve exhaustive digestion ranges from 5 to 10 min. Therefore, with a micro-reactor possessing a volume of 30 nl, a volumetric flow rate of 3–6 nl min^{-1} is required to obtain the required residence time.

Several groups have constructed micro-pumps which are based upon a reciprocating or peristaltic mode of operation and have used piezo-actuators to produce the pumping action.[21–25] In most cases, these pumps use a bimorph which bends when a voltage is applied to the piezo-actuator. By inserting valves into the device, the pump can operate continuously with the volumetric pumping rate determined by the frequency of the driving voltage to the pump chamber. Unfortunately, many of these can operate only at low loading pressures and pump at volume flow rates in the μl min^{-1} range. Also, since the pumping action is based on a reciprocating process, pump pulsations may be evident which could present problems when used in particular applications, *e.g.*, in micro-chromatographic systems where the detector is sensitive to such noise sources.

In this paper, we describe the construction and operational characteristics of a computer-controlled mechanical pump constructed from a piezoelectric actuator (PA), pivot lever and micro-syringe (see Fig. 2). By applying a voltage to the PA, the crystal can be expanded pushing the plunger of the micro-syringe, causing fluid displacement. The expansion of the PA is amplified by means of the pivoted lever, which provides a higher volume displacement per pump stroke. The volumetric flow rate is controlled by specifying the slope on the driving voltage ramp to the PA. Owing to the precise positioning capabilities of the PA, low nl min^{-1} volumetric flow rates can be generated with this device, making it appropriate for fluid pumping in miniaturized chemical analysis systems. In addition, we discuss the micro-fabrication of a diffuser–nozzle system which would allow automatic refilling of the syringe pump without requiring disconnection of the pump from the supply source and the chemical analysis system to which it is interfaced.[26] Recently, several groups have shown that the diffuser–nozzle geometry is a viable choice for valveless operation in micro-mechanical-based pumps using reciprocating type action.[27–30] The diffuser–nozzle system was micro-machined in PMMA using X-ray lithography. The PMMA-based diffuser–nozzle was interfaced to the syringe pump using small diameter fused silica capillary tubes of 50 μm od and 20 μm id.

Experimental

Construction of PA pump

In Fig. 2 is shown a schematic diagram of the micro-pump. All components were mounted on a Plexiglas stage (14.0 × 8.0 × 1.3 cm). The expansion of the PA (Model P-178.50, from Polytec PI, Costa Mesa, CA, USA) was controlled by a computer (Gateway 2000, P5-120) equipped with a 12-bit analog output voltage (0 to ±10 V, dc) from a multi-function I/O board (Model AT-MIO-16XE-50, National Instruments, Austin, TX, USA). The maximum linear displacement for this PA was stated to be 80 μm by the manufacturer when a voltage of −1000 V (negative polarity) was applied from a high voltage power source (Model K10N, from Emco High Voltage, Sutter Creek, CA, USA) which was driven by the output of the DAC. With 4096 (12-bit) step resolution over 10 V (2.44 mV per step), the minimum linear displacement of the PA was 19.5 nm per step (assuming a total linear expansion of 80 μm). The piezo-expansion was amplified using an in-house constructed lever (5.8 × 1.5 × 0.64 cm) and a pivot. The lever sits horizontally on a 0.8 mm thick × 2.5 mm id × 12.0 mm od copper disk that surrounds the pivot and can move without touching any part of the Plexiglas stage. The PA was placed in a rectangular slot (8.1 × 1.8 × 0.4 cm) made on the Plexiglas stage such that the center of the front face of the PA head was butted against the tip of one arm (A-1, see Fig. 2) of the lever. As shown in Fig. 2, the distance between A-1 and the center of the pivot was 5.0 mm, whereas the distance between the center of the pivot and the second arm (A-2) of the lever was 50.0 mm. A spring (S-1) maintained contact between A-1 and the PA head. A micro-syringe (gas-tight, Model RN80230, from Hamilton, Reno, NV, USA) made of glass was situated horizontally on the Plexiglas stage and mounted (at a right-angle with respect to the long axis of the lever) on a drilled slot in this stage. Another spring (S-2)

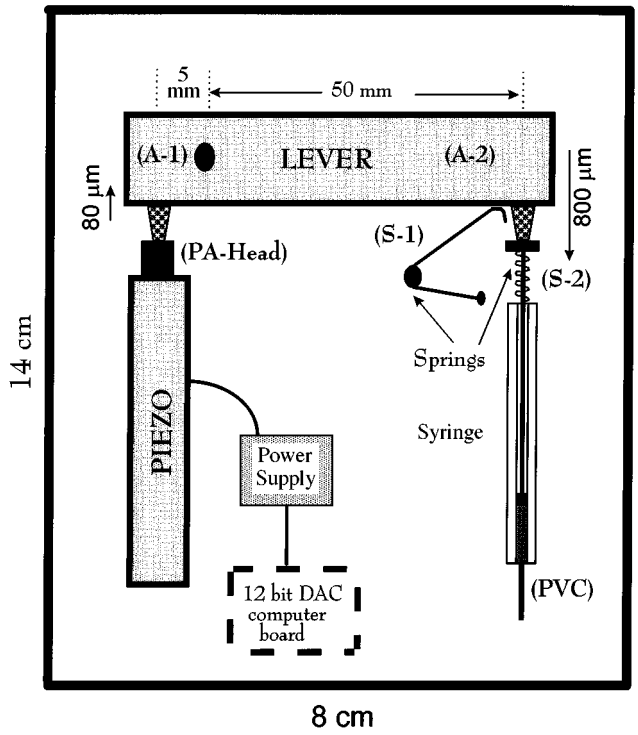

Fig. 2 Schematic representation of the piezo-driven micro-syringe pump.

maintained contact between A-2 of the lever and the syringe plunger. The syringe was connected directly to a fused silica capillary (Polymicro Technologies, Phoenix, AZ, USA) with 2.0 cm × 0.010 in id poly(vinyl chloride) (PVC) tubing (Elkay Products, Shrewsbury, MA, USA).

Measurement of absolute expansion of PA

In order to measure the absolute expansion of the PA and subsequent amplification by the lever, one end of a short piece of fused silica capillary (20 cm × 150 μm od) was attached to the PA head and A-2. The respective expansions were determined by focusing the other end of the capillary under a stereomicroscope (100× magnification, Optiphot-2 microscope, Nikon, Tokyo, Japan) equipped with a CCD video camera and monitored by measuring the movement of this capillary on a calibrated TV screen. The small size of the capillary (low mass) minimized the loading back-pressure on the PA.

Measurement of absolute flow rates

To measure the absolute linear fluid velocity under pump operation (applied voltage), the micro-syringe was filled with a suspension of 0.0005% uniform latex micro-beads (0.203 μm polystyrene micro-spheres, Duke Scientific, Palo Alto, CA, USA) in water. Fused silica capillaries of various lengths were connected to the syringe and movement of the latex beads through a small segment of the capillary window was monitored under the microscope. A window for optical viewing was made by removing about a 1.0 cm portion of the polyimide coating situated about 20 cm from the capillary inlet. The entire capillary was filled with the bead solution manually from the syringe. Care was taken to avoid hydrostatic flows generated by a height difference between the two ends of the capillary causing siphoning action. A timer was used to record the time necessary for the beads to travel through the known viewing segment of the capillary when various voltage ramps were applied to the PA. Since beads were chosen randomly throughout the internal diameter of the capillary tube, the stated flow velocities represent the average linear flow rate of the parabolic flow profile produced by this pressure driven system.

Laser-induced fluorescence determination of flow stability

The flow stability was determined using laser-induced fluorescence (LIF) signals by flowing a solution of 50 nM fluorophoric dye (IR-144, from Kodak Chemicals, Rochester, NY, USA). Owing to the photobleaching experienced by a fluorogenic dye when flowing into a focused laser beam with high irradiance, the fluorescence signal becomes a sensitive probe of flow rate.[31,32] LIF was performed using a 750 nm diode laser (GaAlAs) as the excitation source. This beam was focused on to a 75 cm long multimode glass fiber [50 μm core, 125 μm cladding, 0.30 numerical aperture (NA), from 3M (St. Paul, MN, USA)] with a 20× microscope objective. The distal end of the fiber was situated in close proximity to the observation window of a 10 cm (100 μm id × 365 μm od) fused silica capillary which was affixed to a laboratory made Plexiglas capillary holder. The fluorescence was collected at right-angles (with respect to the laser light) with a 40× (0.85 NA) microscope objective and imaged on to a slit serving as a spatial filter to reduce the amount of scattered photons generated at the air–glass and glass–liquid interfaces of the capillary from reaching the photon transducer. The fluorescence was further isolated from the scattering photons by a 780 nm (±10 nm) bandpass filter and a 780 nm long pass filter and finally focused on to the photoactive area of the detector (single photon avalanche detector, EG&G Optoelectronics, Vaudrieulle, Canada) with another microscope objective (20×). The fused silica capillary was filled with a 50 nM solution of IR-144 fluorescent dye solution (Kodak Chemicals) and connected to the pump.

Construction of diffuser–nozzle system

The principle operational modes of the diffuser–nozzle system is depicted in Fig. 3(A). There are basically two modes of operation, pump supply and pump delivery. During pump supply, the plunger of the syringe pump is retracted, causing sample to fill the pump chamber. During the pump delivery mode, the sample in the pump chamber is delivered to the chemical analysis device. The proper direction of fluid flow during the appropriate pump cycle is determined by two elements, a diffuser and nozzle, which have different pressure drops across them causing maximum flow from one port (diffuser) and minimizing the flow in the other (nozzle). For optimum performance, the pressure drop across the diffuser should be much less than that for the nozzle so that the majority of the solution movement occurs preferentially through the diffuser. The pressure drop across the diffuser (ΔP_d) and nozzle (ΔP_n) can be calculated from[26]

$$\Delta P_d = \frac{\rho v_d^2}{2} \xi_d \quad (1)$$

$$\Delta P_n = \frac{\rho v_n^2}{2} \xi_n \quad (2)$$

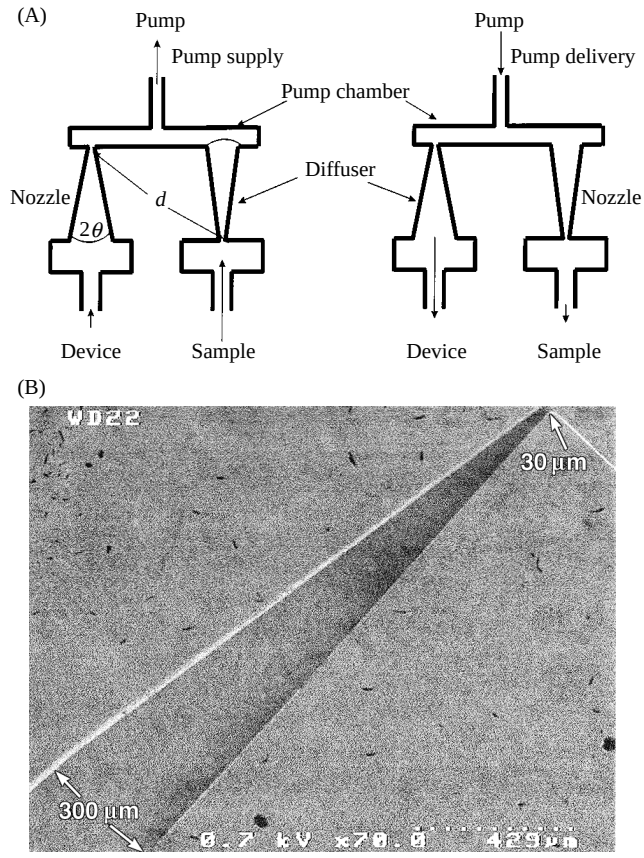

Fig. 3 (A) Operational modes of diffuser–nozzle system. The arrows represent the direction of fluid flow and the magnitude of fluid flow through the device during operation. (B) Scanning electron micrographs of the diffuser–nozzle system micromachined into PMMA using X-ray lithography. The channels were machined to a depth of 50 μm.

where ρ is the density of the solution, ν is the linear flow velocity through the narrowest part of the diffuser or nozzle element and ξ is the pressure loss coefficient. To achieve efficient filling of the pump chamber $\xi_d/\xi_n > 1$, which can be accomplished by minimizing the pressure loss coefficient associated with the diffuser.[33] The pressure loss coefficients depend on a number of design parameters associated with the diffuser and the general topology of the diffuser (flat-walled *versus* conical). For a flat-walled diffuser, the minimum pressure loss occurs in a flow regime classified as transitory stall, where flow separation occurs at the wall of the diffuser. The physical dimensions of the diffuser which must be considered in order to operate in this regime are 2θ and the ratio, *L*/*d*, where these dimensions are defined in Fig. 3(A). In the present case, $L/d = 41$ and $2\theta = 8°$, which put the diffuser in the transitory stall regime.

The required channels were machined into the PMMA substrate using X-ray lithography following previously described procedures.[20,34–36] Briefly, an optical mask containing the required device topography was situated on a 5 cm square piece of PMMA which was coated with a 5 nm layer of Au–Cr, which served as a plating base, and a positive resist. After UV exposure, the resist was developed and a thick overlayer of Au (3 μm) was applied electrolytically to the developed areas to serve as the X-ray absorber during exposure. After the required Au layer was applied to the device, the remaining resist was removed and the device was placed in the X-ray beam and exposed to soft X-rays at our Center for Advanced Microstructure and Device facility. After exposure, the PMMA substrate was developed to remove exposed PMMA and then, after thorough cleaning, another piece of PMMA was thermally bonded to the diffuser–nozzle device. In Fig. 3(B) is shown a scanning electron micrograph of the micromachined PMMA. The depth of the channels was found to be 50 μm and the narrowest portion of the diffuser–nozzle was 30 μm with the widest part being 300 μm. Owing to the ability to machine in PMMA using X-rays with high aspect ratios, the channel topography in the diffuser–nozzle was considered to be flat-walled and not conical.

After sealing the PMMA top sheet to the diffuser–nozzle, small diameter capillary tubes were inserted into the three ports of the diffuser–nozzle, one interfaced to the syringe pump, the second to the sample supply and the third port to the chemical analysis system. The capillary tubes were of 20 μm id and 40 μm od. These capillary tubes were inserted into the narrow PMMA channels by placing the tube on an *XYZ* micropositioner and then carefully inserting the capillary tube into the PMMA channel using an optical microscope for visual inspection. Once the capillary tube had been properly inserted into the device, it was sealed to it using epoxy.

Results and discussion

Piezo-pump characteristics

The PA used in the fabrication of the pump was made from a thin-layered ceramic stack which allowed greater expansion. The translator expands between the casing and the magnetic top piece (PA head). This particular piezo-stack is expected to produce a linear expansion of 80 μm and operate with a maximum pushing force of 2000 N (pressure = 6.37×10^6 Pa for head area of 3.14 cm^2). Our microscopic observations revealed that the maximum expansion of the PA was 72 μm at an applied voltage of −1000 V when approximately 68.9 Pa (0.01 psi) back-pressure was loaded on to the syringe. This amounts to a 10% loss in linear displacement when little or no load was applied against the PA. The main purpose of using the pivoted lever was to amplify the PA expansion in order to permit higher volume displacements per pump stroke. The output displacement of the single-lever expansion unit was determined to be 648 μm, which resulted in an expansion gain of 9.0.

Expansion and amplification of PA movement during voltage ramp

The absolute expansion of the piezoelectric actuator and its amplification by the pivoted lever (with no load) were monitored as a function of a linear voltage ramp. A plot of the observed PA and PA–lever linear displacement with respect to the progression of the voltage ramp is shown in Fig. 4. In both the amplified and non-amplified linear displacements, no expansion was observed until the applied voltage reached about −100 V. As can be seen from this plot, the displacement of the PA was fairly linear with applied voltage except at low applied voltages (−100 to −300 V) and then at the high end of the voltage ramp also (−800 to −1000 V). This type of expansion profile can be expected owing to hysteresis effects from this type of piezoelectric translator, particularly when operated without a position sensor. To obtain a linear expansion of the PA, a non-linear voltage ramp can be used to compensate for these effects. It can also be observed from Fig. 4 that the amplified displacement by the lever tracked the displacement of the PA without amplification fairly well with non-linearities at the high and low ends of the applied voltage ramp. Assuming a ninefold amplification factor by the lever, it can be seen from this plot that the amplification is less than ninefold below an applied voltage of −200 V and then exceeds ninefold above an applied voltage of −600 V.

Pump flow profile during voltage ramp

The volumetric flow rate (nl min^{-1}) is basically a function of two parameters: the slope of the applied voltage ramp (V s^{-1}) and the diameter of the micro-syringe. Since we used a linear voltage ramp, the pivoted lever amplified expansion was expected to be dependent on the absolute expansion behavior of the PA and the load pressure also. The flow rate of latex beads was followed in a 2.56 mm long window of a 30 cm × 50 μm id fused silica capillary (the viewing window was in the middle of the capillary). Based on our microscopic studies, no pumping action was seen until the voltage reached approximately −100 V with a load pressure (Δ*P*) of 0.22 psi (1.5×10^3 Pa), which was calculated using the expression

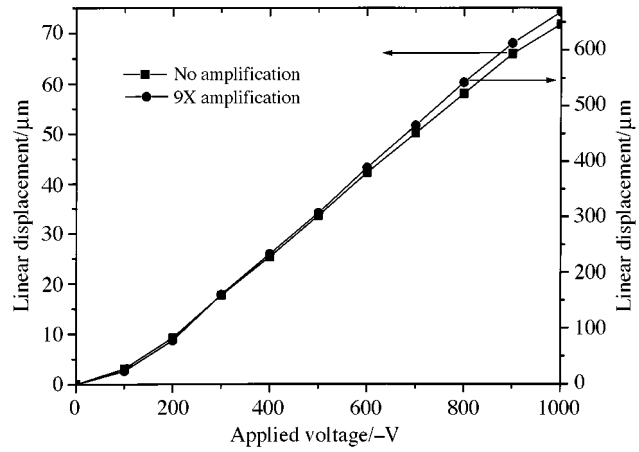

Fig. 4 Linear displacement of piezo-head, non-amplified (squares) and amplified (circles), *versus* applied voltage. The linear displacement was determined by placing a short piece of capillary tube against the PA head and then monitoring the movement of the capillary tube under a stereomicroscope with a video screen that was calibrated.

$$\Delta P = \frac{8LQ\eta}{\pi R^4} \quad (3)$$

where L is the length of the capillary tube (m), Q is the volume flow rate ($m^3\ s^{-1}$), η is the solution viscosity (Pa s) and R is the radius of the capillary (m). In this case, the solution viscosity was assumed to be near that of pure water (1 cP or 0.001 Pa s). It should also be noted that owing to the amplification by the pivoted lever, this load pressure is back-amplified to the PA so that the actual load pressure at the PA head is 1.98 psi (1.35×10^4 Pa). In addition, this load pressure was calculated at the highest volume flow rate investigated (47.8 nl min^{-1}) and is expected to decrease at the lower volume flow rates. The observed flow patterns at three ramp speeds are shown in Fig. 5. Qualitatively, we did not notice any pulsing movement of the microbeads resulting from pump steps in the ramp-speed range 0.25–4.4 V s^{-1} in this 50 μm id capillary. However, in these experiments we did observe the beads close to the wall moving more slowly than those in the center of the capillary owing to the parabolic nature of the laminar flow. As is apparent from Fig. 5, the volume flow rate requires a fixed time period (applied voltage) to reach a constant value with the duration dependent upon the ramp rate (*i.e.* load pressure). For example, at a ramp rate of 1.96 V s^{-1}, the volume flow rate does not become constant until an applied voltage of about −400 V is reached, whereas for a voltage ramp of 0.49 V s^{-1}, the volume flow rate reaches a constant value at an applied voltage of approximately −150 V. As shown in the inset in Fig. 5, the volume flow rate was linear (r = 0.9998) with the applied linear voltage ramp over the range investigated (0.49–1.96 V s^{-1}).

Effect of applied back-pressure

The dependence of liquid flow rate on applied back-pressure at different voltage ramps was determined from microscopic experiments. A 2.0 m × 20 μm id fused silica capillary was connected to the pump and filled with a latex bead solution. The liquid was pumped through the capillary at different flow rates which were controlled by varying the slope of the applied voltage ramp to the PA. This operation was repeated after reducing the length of the capillary in 0.3 m increments. The observed flow rates increased linearly with increase in the slope of the voltage ramps for this series of capillaries, which is illustrated in Fig. 6(A). If the load pressure did not exert a perturbation on the volume flow rate, then these lines should exhibit similar slopes, independent of tube length. However, as can be seen from this graph, deviations are observed at high pumping rates (large pressure drops) for different lengths of capillaries, indicating that the volume flow rate will show some dependence on load pressure. The effect of pressure drop across the capillary on the observed flow rate is presented in Fig. 6(B), in which the pressure was calculated from eqn. (3). As can be seen, the volumetric flow rate decreased with increasing pressure drop. Given a fixed diameter and length of capillary, the magnitude of this effect (slope of volume flow rate *versus* load pressure) increases with increasing pumping rate since the load pressure also depends on the volume flow rate.

These effects can easily be rationalized based on the fact that the PA can be considered to act as an elastic body with a given stiffness and a changing load during the expansion. The load pressure changes during the expansion since the flow velocity increases during each voltage step, which results in reductions of expansion under load conditions (ΔL). This loss can be determined from the expression

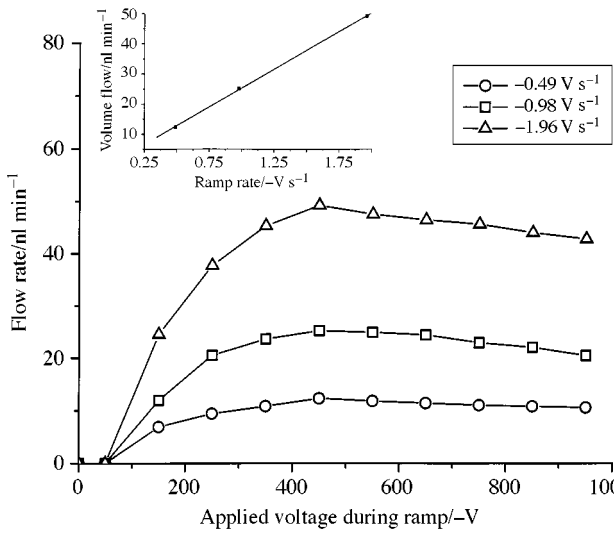

Fig. 5 Volume flow rate *versus* applied voltage to the amplified PA head. The linear velocity was determined by observing the movement of the micro-beads in water moving through a 30 cm × 50 μm id capillary tube using a stereomicroscope. The volume flow rate was calculated by multiplying the observed linear velocity by the cross-sectional area of the capillary tube.

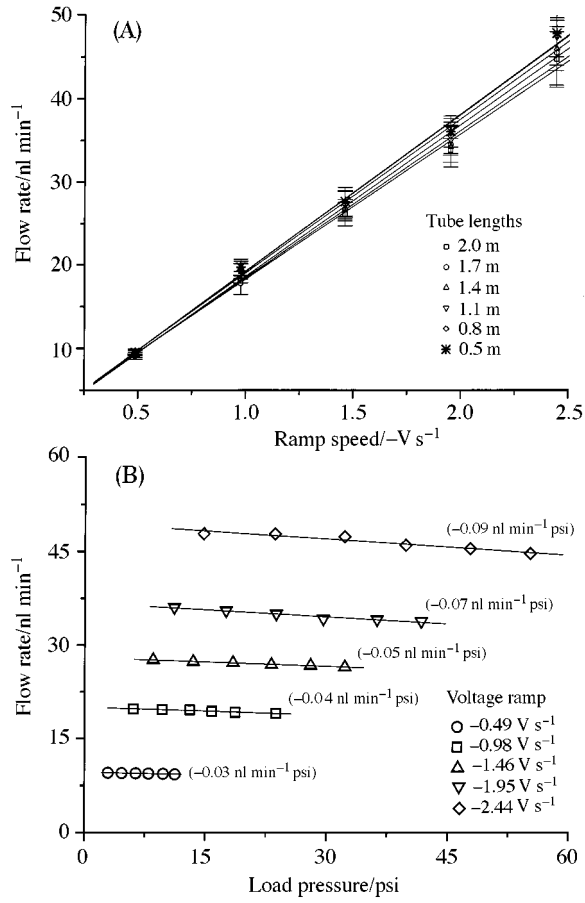

Fig. 6 (A) Volume flow rate as a function of ramp speed (V s^{-1}) for 20 μm id tubes of various lengths. The lengths of the capillary tubes were changed in 0.3 m increments so as to alter the load pressure on the PA head. (B) Volume flow rate *versus* load pressure at five different ramp speeds (V s^{-1}). If the volume flow rate was not dependent on load pressure, then the slopes of these plots should be zero. The load pressure shown here does not account for the amplification factor associated with the pivoted lever. Therefore, the actual load pressure at the PA head should be multiplied by nine. The volume flow rate was calculated using the same procedure as described in Fig. 4.

$$\Delta L = L_0 \frac{c_T}{c_T + c_S} \quad (4)$$

where L_0 is the linear displacement under no load conditions (72 μm), c_T (N μm^{-1}) is the stiffness of the PA (45 N μm^{-1}) and c_s (N μm^{-1}) is the stiffness or spring constant of the load. For a capillary of 2.0 m × 20 μm id and a pump volume flow rate of about 47 nl min^{-1}, the pressure drop at the PA head is 513 psi (57 psi × 9, where 9 is the amplification factor of the pivoted lever) or 3.54 × 10^6 Pa. This results in a value of c_s = 15.4 N μm^{-1}. Under these load conditions, the actual linear expansion is 54 μm or 13.6 nm per step (12-bit DAC) compared with 17.6 nm per step under no-load conditions. At a driving voltage ramp of 2.44 V s^{-1} the volume flow rate with this load was calculated to be 55.5 nl min^{-1}, which compared favorably with the observed 47.8 nl min^{-1} measured under these load conditions [see Fig. 6(B)]. Under no-load operation, the volume flow rate expected would have been 74.6 nl min^{-1}.

Flow stability

In order to examine the stability of the pump when operated at low volume flow rates, a dye solution was pumped through a 100 μm id capillary tube and the fluorescence was monitored during the driving voltage ramp at three different ramp rates. When the dye molecules travel through an intense Gaussian laser beam, the integrated fluorescence intensity depends on the photoalteration parameter (F), which was determined using the expression[31]

$$F = P\Phi_d\sigma/(\pi^{1/2}\omega\nu) \quad (5)$$

where P is the average laser irradiance (photons s^{-1}), Φ_d is the dye photodestruction quantum efficiency, defined as the probability that a molecule photodegrades once in the excited state, σ is the absorption cross-section (cm^2), ω is the 1/e^2 laser beam radius (cm) and ν is the linear flow velocity of the fluorescent dye molecule (cm s^{-1}). As can be seen from this expression, F depends inversely on the linear flow velocity and hence will affect the integrated fluorescence intensity. Therefore, monitoring the fluorescence intensity will be a sensitive indicator of flow fluctuations produced by the pump. However, it should be pointed out that only under the conditions of $0.1 \leqslant F \leqslant 100$ does the integrated fluorescence depend directly on the photoalteration parameter. When $F < 0.1$, no dye bleaches during its travel through the beam, and when $F > 100$, all dye molecules are immediately bleached upon entering the sampling volume. In the present case for the dye used in these experiments (IR-144), P = 1.88 × 10^{16} photons s^{-1} (5 mW at 750 nm), σ = 2.4 × 10^{-16} cm^2, ω = 25 × 10^{-4} cm, Φ_d = 9 × 10^{-7} and variation of ν from 1.9 × 10^{-5} to 8.2 × 10^{-4} cm s^{-1} resulted in a photoalteration parameter which ranged from 47 to 1.1. The fluorescence intensity as a function of three different volumetric flow rates is displayed in Fig. 7. As can be seen, the average intensity is a function of the flow rate, indicating that the photoalteration parameter is within the range where the fluorescence intensity does depend upon the linear flow velocity. Careful inspection of the data when the pump has reached a level where the average fluorescence intensity is constant demonstrates the lack of large fluctuations in the intensity which could arise from pulsations in the pumping action. However, there is some noise superimposed on these traces, most of which arises from Poisson noise (shot noise) in the counting experiment. This is particularly evident at the very low pumping rate (9.18 nl min^{-1}) where the average fluorescence intensity is low and the degree of photobleaching is high (F = 47).

Conclusions

We have fabricated a micro-syringe pump which consisted of a piezo-pusher and pivoted lever for amplifying the displacement of the PA. This pump can deliver volume flow rates in the low nl min^{-1} range, even under the conditions of high load pressures where the peristaltic pumps may display difficulties. Since the pump will operate under high loads, it will be an important device for micro-fluidic applications where solutions must be pumped through narrow bore channels. In addition, the low volume flow rates that are achievable will allow manipulation of fluids in narrow channels which require long residence times, such as in micro-chromatographic techniques or micro-based flow injection analysis. Another advantage associated with the present device is that pump-dependent noise resulting from pulsations is absent. However, a difficulty associated with this pump in its present format is the limited volume it can deliver per pump stroke. At a pump volume of 560 nl and a volume flow rate of 9.2 nl min^{-1}, it can effectively operate for 60 min before requiring to be refilled, but at a flow rate of 368 nl min^{-1} the pump can operate for only 1.5 min. Another potential problem is the ruggedness of the device, owing to the need for the sophisticated pivoted lever system. An alternative format for amplifying the linear displacement of the PA could reduce this difficulty, *e.g.*, the implementation of a pulley system. In order to refill the pump automatically without requiring disconnection of the pump from the chemical analysis system, a diffuser–nozzle device was micromachined into PMMA to create a low volume pump chamber and channel network to allow ease of use. The micromachined diffuser–nozzle contains no moving parts and can allow directing flows in hydrodynamically driven systems. However, it should be pointed out that during operation of the diffuser–nozzle for pump refilling, discontinuities in the flow do result.

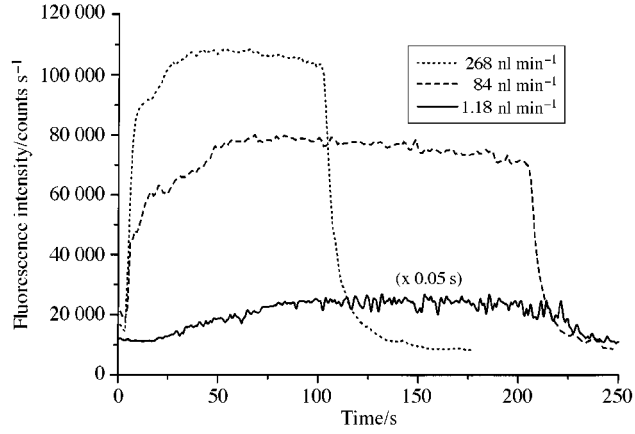

Fig. 7 Pump stability at three different volume flow rates. The flow stability was determined by monitoring the fluorescence produced by the dye IR-144. The fluorescence was excited with 5 mW of laser power at 750 nm. The fluorescent dye was dissolved in methanol at a concentration of 50 nM

The authors thank the Whitaker Foundation for financial support of this reseach. They also like to thank Professor Robin McCarley for helpful discussions during the course of this work.

References

1 Rothman, L. D., *Anal. Chem.*, 1996, **68**, 587R.
2 Lunte, C. E., Scott, D. O., and Kessinger, P. T., *Anal. Chem.*, 1991, **63**, 773A.
3 Harrison, D. J., Fluri, K., Seiler, K., Fan, Z., Effenhauser, C. S., and Manz, A., *Science*, 1993, **261**, 895.
4 Effenhauser, C. S., Manz, A., and Widmer, H. M., *Anal. Chem.*, 1993, **65**, 2637.
5 Harrison, D. J., Glavina, P. G., and Manz, A., *Sens. Actuators B*, 1993, **10**, 107.

6 Fan, Z. H., and Harrison, D. J., *Anal. Chem.*, 1994, **66**, 177.
7 Jacobson, S. C., Hergenroder, R., Koutny, L. B., Warmack, R. J., and Ramsey, J. M., *Anal. Chem.*, 1994, **66**, 1107.
8 Jacobson, S. C., Hergenroder, R., Koutny, L. B., and Ramsey, J. M., *Anal. Chem.*, 1994, **66**, 1114.
9 Effenhouser, C. S., Paulus, A., Manz, A., and Widmer, H. M., *Anal. Chem.*, 1994, **66**, 2949.
10 Jacobson, S. C., Koutny, L. B., Hergenroder, R., Moore, A. W., and Ramsey, J. M., *Anal. Chem.*, 1994, **66**, 3472.
11 Seiler, K., Fan, Z. H., Fluri, K., and Harrison, D. J., *Anal. Chem.*, 1994, **66**, 3485.
12 Woolley, A. T., and Mathies, R. A., *Proc. Natl. Acad. Sci. USA*, 1994, **91**, 11 348.
13 Jacobson, S. C., Moore, A. W., and Ramsey, J. M., *Anal. Chem.*, 1995, **67**, 2059.
14 Effenhauser, C. S., Manz, A., and Widmer, H. M., *Anal. Chem.*, 1995, **67**, 2284.
15 Woolley, A. T., and Mathies, R. A., *Anal. Chem.*, 1995, **67**, 3676.
16 Raymond, D. E., Manz, A., and Widmer, H. M., *Anal. Chem.*, 1996, **68**, 2515.
17 Jacobson, S. C., and Ramsey, J. M., *Anal. Chem.*, 1996, **68**, 720.
18 Fluri, K., Fitzpatrick, G., Chiem, N., and Harrison, D. J., *Anal. Chem.*, 1996, **68**, 4285.
19 Schwer, C., and Kenndler, M. G., *Anal. Chem.*, 1991, **63**, 1801.
20 Ford, S. M., Kar, B., McWhorter, S., Davies, J., Soper, S. A., Klopf, M., Calderon, G., and Saile, V., *J. Microcol. Sep.*, in the press.
21 van Lintel, H. T. G., van de Pol, F. C. M., and Bouwstra, S., *Sens. Actuators*, 1988, **15**, 153.
22 van de Pol, F. C. M., Wonnink, D. G. J., Elwenspoek, M., and Fluitman, J.H. J., *Sens. Actuators*, 1989, **17**, 139.
23 Smits, J. G., *Sens. Actuators*, 1990, **21**, 203.
24 Schomburg, W. K., Fahrenberg, J., Maas, D., and Rapp, R., *J. Micromech. Microeng.*, 1993, **3**, 216.
25 Korenaga, T., Zhou, X., Moriwake, T., Muraki, H., Naito, T., and Sanuk, S., *Anal. Chem.*, 1994, **66**, 73.
26 Stemme, E., and Stemme, G., *Sens. Actuators A*, 1993, **39**, 159.
27 Olsson, A., Enoksson, P., Stemme, G., and Stemme, E., *J. Micromech. Microeng.*, 1995, **6**, 87.
28 Heschel, M., Mullenborn, M., and Bouwstra, S., *J. Microelectromech. Syst.*, 1997, **6**, 41.
29 Olsson, A., Enoksson, P., Stemme, G., and Stemme, E., *J. Microelectromech. Syst.*, 1997, **6**, 161.
30 Olsson, A., Larsson, O., Holm, J., Lundbladh, L., Ohman, O., and Stemme, G., *Sens. Actuators A*, 1998, **64**, 63.
31 Mathies, R., Oseroff, A. R., and Stryer, L., *Proc. Natl. Acad. Sci. USA*, 1976, **73**, 1.
32 Soper, S. A., Nutter, H. L., Keller, R. A., Davis, L. M., and Shera, E. B., *Photochem. Photobiol.*, 1993, **57**, 972.
33 White, F. M., *Fluid Mechanics*, McGraw-Hill, New York, 1986, pp. 348–352.
34 Vladimirsky, Y., Vladimirsky, O., Saile, V., Morris, K. J., and Klopf, J. M., *Proc. SPIE*, 1995, **2621**, 399.
35 Vladimirsky, Y., Vladimirsky, O., Saile, V., Morris, K. J., and Klopf, J. M., *Proc. SPIE*, 1995, **2437**, 391.
36 Ford, S. M., Davies, J., Kar, B., Owens, C. V., Klopf, M., Calderon, G., Saile, V., and Soper, S. A., *Anal. Chem.*, submitted for publication.

Paper 8/00052B
Received January 2, 1998
Accepted March 17, 1998